ELSEVIER

Chemical Engineering Journal 140 (2008) 414–423

Chemical Engineering Journal

www.elsevier.com/locate/cej

A model for the pressure balance of a low density circulating fluidized bed

Enrico Grieco, Luca Marmo *

Politecnico di Torino, c.so Duca degli Abruzzi 24, 10129 Torino, Italy

Received 14 June 2007; received in revised form 30 October 2007; accepted 9 November 2007

Abstract

The pressure balance along the solid circulation loop of a circulating fluidized bed equipped with a solid flux regulating device has been modelled and the influence of the pressure balance on the riser behaviour has been predicted.

The solid circulation loop has been divided into many sections, where the pressure drop was calculated independently: riser, cyclone, standpipe, control device and return duct. A new theoretical model, that is able to predict the pressure losses in the return path of the solid from the standpipe to the riser, has been built. A new correlation for cyclone pressure loss with very high solid loads has been found on the basis of experimental data.

The pressure loss in the riser has been calculated by imposing the closure of the pressure balance, $\Sigma \Delta P = 0$. Once the riser pressure drop had been calculated, the holdup distribution along the riser was obtained by imposing a particular shape of the profile, according to the different fluid-dynamics regimes (fast fluidization or pneumatic transport). In the first case, an exponential decay was imposed and the bottom holdup was adjusted to fit the total pressure drop, in the second case, the height of the dense zone was instead varied.

The experimental data was used to develop the sub-models for the various loop sections have been obtained in a 100 mm i.d. riser, 6 m high, CFB. The solid was made of Geldart B group alumina particles. The tests were carried out with a gas velocity that ranged between 2 and 4 m/s and a solid flux that ranged between 20 and 170 kg/m^{2}s. A good agreement was found between the model and experimental data.
© 2007 Elsevier B.V. All rights reserved.

Keywords: Circulating fluidized bed; Pressure balance; Fast fluidization

1. Introduction

Circulating fluidized beds are used in many applications in the process industry as fast catalytic reactions as well as for the combustion of solids. The control of the solid circulation rate in CFB plants can be achieved by varying the pressure losses in the return leg of the solid from the standpipe bottom to the riser. A typical control device consists of a valve (mechanical or not) placed somewhere below the standpipe. The valve absorbs a part of the pressure that has built up in the standpipe due to the solids head. By varying the pressure absorbed by the control device, the solid circulation rate changes to adjust the whole pressure balance of the loop. In the case of a mechanical valve (slide valve, butterfly valve) the change in the pressure drop of the control device is obtained by reducing the section where the solid can flow.

Lei and Horio [1] proposed a comprehensive model for the calculation of the pressure balance in the loop of a circulating fluidized bed equipped with a regulating valve. In this case the whole pressure balance was used to take into account the gas flowing in the return leg, in order to obtain a better modelling of the riser. Cheng et al. [2,3], Bai et al. [4] and Lim et al. [5] calculated the solid circulation rate on the basis of the loop pressure balance. Rhodes and Geldart [6] used the loop pressure balance to determine the quantity of the solid in the standpipe. Kim et al. [7] and Yang [8] used a loop pressure balance to calculate the height of the dense zone at the bottom of a fast fluidized riser, equipped with an *L*-valve and an abrupt exit from the riser.

This paper shows how it is possible to use the whole pressure balance to predict the behaviour of the riser even in the transport regime, as sufficient accurate sub-models for the different contributions of loop parts are available. The loop pressure balance corresponds to Eq. (1):

$$\Delta P_{\mathrm{R}} = \Delta P_{\mathrm{SP}} - \Delta P_{\mathrm{cy}} - \Delta P_{\mathrm{RD}} - \Delta P_{\mathrm{val}} - \Delta P_{\mathrm{UD}} \quad (1)$$

* Corresponding author. Tel.: +39 11 5644697; fax: +39 11 5644699.
E-mail address: luca.marmo@polito.it (L. Marmo).

1385-8947/$ – see front matter © 2007 Elsevier B.V. All rights reserved.
doi:10.1016/j.cej.2007.11.018

Nomenclature

a	decay factor for the solid holdup in the riser
A	cross-section (m^2)
d_p	particle diameter (m)
D	diameter (m)
D_b	butterfly valve diameter (m)
f	friction contribution to the riser ΔP (Pa/m)
ΔP	pressure loss in a section of the solid circulation loop (Pa)
g	gravitational acceleration ($g = 9.81$ m/s^2)
G_S	solid flux (kg/m^{2}s)
L	length of a particular section of the solid circulation loop (m)
$\dot{m}$	mass flow (kg/s)
m	mass (kg)
n	number of control volumes for the calculus of the valve
p	perimeter (m)
Re	particle Reynolds number ($U_s \cdot d_p \cdot \rho_g/\mu$)
U	superficial velocity (m/s)
U_t	particle terminal velocity (m/s)
v	velocity (m/s)
$\dot{V}$	volumetric flow rate (m^3/s)
vt	thickness of the control volumes for the calculus of the valve (m)
W	solid inventory (kg)
x	distance from the butterfly valve centre (m)
z	height from the riser bottom (m)
z_d	height of the dense zone in the riser (m)
β	butterfly rotation angle with respect to the closed position (°)
γ	butterfly valve correction factor
ε	void fraction
ε_p	solid fraction
μ	gas viscosity (kg/ms)
μ_e	cyclone load ratio
ρ	density (kg/m^3)

Subscripts

0	position corresponding at a distance of $0.5D_{RD}$ from the control valve centre
cs	cross-section
cy	cyclone
f	friction
g	gas phase
mf	minimum fluidization
p	particle
pb	packed bed
R	riser
RD	duct connecting the standpipe bottom with the control valve
SP	standpipe
SRL	secondary solid return leg (from the second cyclone to the standpipe bottom)
t	total, in the whole plant
s	solid phase
sl	slip between the gas and solid
UD	upper duct connecting the riser top to the cyclone
val	butterfly valve
∞	height above the transport disengaging height

where in order to determinate riser pressure drop (ΔP_R), it is necessary to calculate the pressure drop in the standpipe (ΔP_{SP}), in the cyclone (ΔP_{cy}), in the solids return leg (ΔP_{RD}), in the control valve (ΔP_{val}) and in the duct connecting the top of the riser to the cyclone (ΔP_{UD}).

Lei and Horio [1] and Cheng et al. [2,3] neglected ΔP_{UD} and used the well-known approach proposed in [9] in order to determine the pressure losses in the return leg and to calculate the gas flux. The pressure loss in the valve, ΔP_{val} is generally calculated as a simple function of the geometry and solid circulation rate, then, imposing these pressure losses as being due to the gas flow, it is possible to calculate the gas flow rate as proposed in [10].

Experimental tests were performed on a laboratory scale CFB plant equipped with a butterfly valve which functioned as a solid flux control device. Grieco and Marmo [11] showed that, for such control devices, it is necessary to use a specific correlation that is able to predict pressure losses in the valve. Moreover, the particular geometry of the butterfly valve openings made it necessary to develop a new approach that was able to calculate the gas flow through the openings and the pressure losses in the return duct between the standpipe bottom and the butterfly valve.

According to a classical approach, once ΔP_R is known, the solid holdup in the riser should respect the Eq. (2):

$$\int_0^{z_R} [g \cdot \rho_p(1-\varepsilon) + f]\mathrm{d}z = \Delta P_R \tag{2}$$

where g is the gravity acceleration, ρ_p is the particle density, ε is the void fraction and f is a term taking into account the friction.

The axial holdup profile is then calculated in two different ways, that depend of the fluid-dynamics regime (fast fluidization or pneumatic transport) which are identified on the basis of the Bai–Kato [12] correlation. In this paper, the Wong's model [13] was used, in which the bottom solid holdup was corrected in order to respect the Eq. (2), for the pneumatic transport.

In the case of fast fluidization, the critical parameter is the height of the dense zone, which is determined again by imposing Eq. (2). The dense zone holdup was calculated using the Bai–Kato [14] correlation, the upper zone was assumed to have an exponential reduction of the holdup, therefore the Wong et al. [13] correlation was used for ε_∞ and the Lei–Horio [1] correlation was used for the decay factor (a).

2. Experimental

Experiments were carried out in the circulating fluidized bed shown in Fig. 1. This bed is composed of a 0.1 m i.d., 6 m high

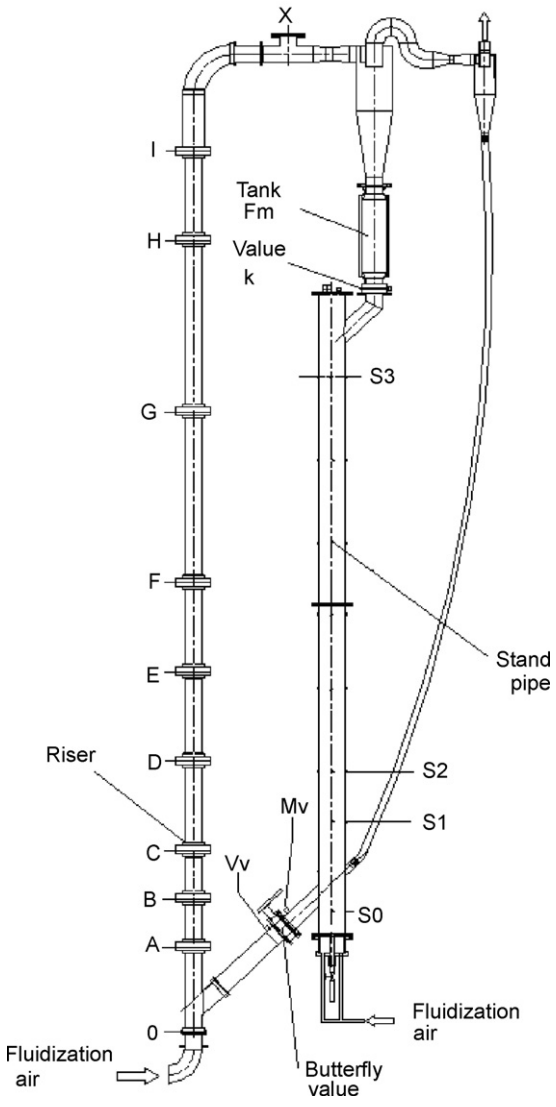

Fig. 1. Scheme of the plant and position of the pressure probes.

riser and a 0.154 m i.d. standpipe. The riser is made of several glass sections of different lengths, the distributor of the fluidization air is a plate with 50 holes, 4 mm diameter, and the discharge occurs through a smoothed exit (0.30 m radius) which leads the air–solid mixture to a couple of cyclones placed in series.

The solids are captured by the first cyclone and then fall through the solid flow rate measuring device. This device consists of a calibrated hopper equipped with a valve at the bottom, whose closure allows the solids to settle in the hopper where the height of the settled powder is then measured. The solid then falls into the standpipe, which is a 0.154 m i.d stainless steel tube that is connected to the riser bottom via an inclined duct (0.1 m i.d.). The duct has an angle of 45° between its axis and the vertical direction. A butterfly valve, which is used as solid circulation rate control device, is located in the middle of this duct (400 mm from the standpipe axis). Secondary fluidization air is fed at the bottom of the standpipe through an air distributor, in order to keep the bed of solids in the return leg fluidized; the air required for the standpipe fluidization is about 12.7 m^3/h.

Several pressure probes are located along the riser and the whole loop through which the solid moves, in order to measure the pressure losses along the circuit; the positions of the probes are shown in Fig. 1, where each letter corresponds to a pressure probe. All the probes were connected to water manometers. The errors connected with the pressure drop measurement are always less than 10 Pa.

In order to obtain detailed pressure profiles along the riser, it was equipped with a mobile pressure probe, that is able to measure the pressure drop between two points 50 cm apart, at any position along the axis of the riser. The probe is made of a thin stainless steel pipe (3 mm diameter, 50 cm length) closed in the centre; a few small holes have been drilled near the two tips, which are connected to two flexible pipes, that are used to transmit the pressure corresponding at each end of the steel probe to a differential manometer.

The flexible pipes are used to drive the pressure probe along the riser axis at the desired height. The lower flexible pipe enters the riser near the bottom, the upper one enters the riser near its top.

Specially conceived seals were realized to allow the flexible pipe to move axially along the riser and hence to locate the probe at the desired position.

The flexible pipes and the probe are much thinner than the riser and introduce very little perturbation to the riser fluid-dynamics.

Two pressure probes were used to sample the butterfly valve pressure drop; one was positioned 6 cm upstream and one 6 cm downstream of the butterfly (Mv and Vv probes). The pressure drop in the duct connecting standpipe bottom to the valve was measured by the S0 and Mv probes.

The solid flux was measured using a manual procedure: the valve (k) located below the calibrated hopper (F_m) was closed, then the time needed to collect a given amount of solid in the hopper was measured.

During this operation, the sold circulation rate decreased slowly, due to the decrease in the height of the powder in the standpipe, which reduces the pressure recovery in the return leg. Hence the value of the solid circulation rate was calculated as the intercept, on the vertical axis, of a graphic that represents the solid flux measured as a function of the amount of solid collected in F_m.

A class B solid according to Geldart [15], was used for the experiments; its properties are shown in Table 1. The particles are made of Al_2O_3.

The experiments were carried out at two different solid inventories equal to 20.1 and 36.3 kg, respectively and at various gas velocities and solid flow rates, which are summarized in Table 1.

3. Modelling

3.1. Pressure drop in the standpipe

In operative conditions, some of the solid inventory is distributed around the plant: in the riser, the return leg duct, and the secondary return leg from the second cyclone. As a consequence when the riser is operated the amount of the solid in the

Table 1
Solid properties and operative conditions

Size range (μm)	25–125	Bulk density (kg/m^3)	~1000
Mean particle diameter (μm)	82	Gas velocity range (m/s)	2–4
Apparent particle density (kg/m^3)	2970	Solid flux (kg/m^{2}s)	20–170
Solid density (kg/m^3)	3330	Solid inventory (kg)	20–36

standpipe (W_{SP}) is lower than the solid inventory. This condition can be described by the mass balance:

$$W_{SP} = W_t - W_{RD} - W_R - W_{SRL} \quad (3)$$

where W_t is the solid inventory, W_{RD}, W_R and W_{SRL} are, respectively, the mass of solid in the return duct, in the riser and in the secondary return leg. If one considers that the height of solid in the standpipe and in the secondary return leg (both fluidized) are the same, Eq. (3) can be rearranged as:

$$W_{SP}\left(\frac{1 + A_{SRL}}{A_{SP}}\right) = W_t - W_{RD} - W_R \quad (4)$$

A_{SP} and A_{SRL} are the cross-section areas of the standpipe and of the duct connecting the second cyclone to the standpipe bottom (see Fig. 1).

According to Lei and Horio [1], Yang [8] and Kim et al. [7], the standpipe pressure drop (ΔP_{SP}) is proportional to the solid inventory present in the standpipe, so combining Eqs. (3) and (4), one obtains:

$$\Delta P_{SP} = g \cdot \frac{W_{SP}}{A_{SP}} = g \cdot \frac{(W_t - W_{RD} - W_R)}{(A_{SP} + A_{SRL})} \quad (5)$$

3.2. Pressure drop in the cyclone

The pressure drop in the cyclone of CFB plants has usually been calculated by means of a simple relation that neglects the contributions of the solid [1,7,16], but in this work a very poor agreement was found between the results of this approach and experimental data. Very poor results were also found with the Martinez–Casal [17] correlation, which also only depends on the gas flux. Even the more complex Muschelknautz and Brunner [18] model led to very poor results (Fig. 2) because it predicts a too little influence of the solid load with respect to the experimental results. The model proposed by Comas et al. [19] required an empirical parameter, but it was still not able to predict the experimental data at high solid loads (Fig. 2): it considers a linear dependence between solid load and the pressure loss, and it leads to an overestimation of the pressure loss at higher solid loads. The reason for the disagreement is likely to be connected to the fact that the correlations were built for very reduced solid loads ($\mu_e \ll 1$), much lower than those corresponding to the normal working conditions of CFB cyclones ($8 < \mu_e < 35$). Also the more recent and detailed models developed by Chen and Shi [20] and by Zhao [21] can't be used for such high solid loads. As a consequence, a new correlation was built that is able to describe the behaviour of the cyclone at high solid loads, on the basis of on purpose experimental tests.

As a result, the correlation corresponding to Eq. (6) was found:

$$\Delta P_{cy} = 0.618 \cdot \rho_g \cdot U_{cy}^2 + (24.54 \cdot U_{cy}^{0.68}) \cdot \mu_e^{0.61} \quad (6)$$

where μ_e, according to [18] and [19], is the load ratio that corresponds to $\dot{m}_{sol}/\dot{m}_{gas}$ and U_{cy} is the gas velocity in the narrowest section of the cyclone inlet duct.

3.3. Pressure drop in the solid circulation rate control valve

In order to apply the approach proposed by Leung and Jones [9] to calculate the gas flow and the pressure drop through the return leg connecting the standpipe bottom to the riser, it is necessary to determine the pressure drop in the solid circulation rate control valve as a function of the solid flow rate. As a first approach, literature correlations found for circular orifices [22–24] or for rectangular orifices [3,25,26], were tested, but Grieco–Marmo [11] showed that these correlations give very poor results when applied to a butterfly valve, where the border effects are much more important than in circular or rectangular orifices. They introduced a correction for Cheng et al. [3] correlation based on a dimensionless parameter γ (see the Eq. (7)), varying between 0 and 1, that is able to take into account the importance of the wet perimeter with respect to the cross-section openings.

$$\gamma = \frac{p_{val,max}/A_{RD}}{p_{cs}/A_{cs}} \quad (7)$$

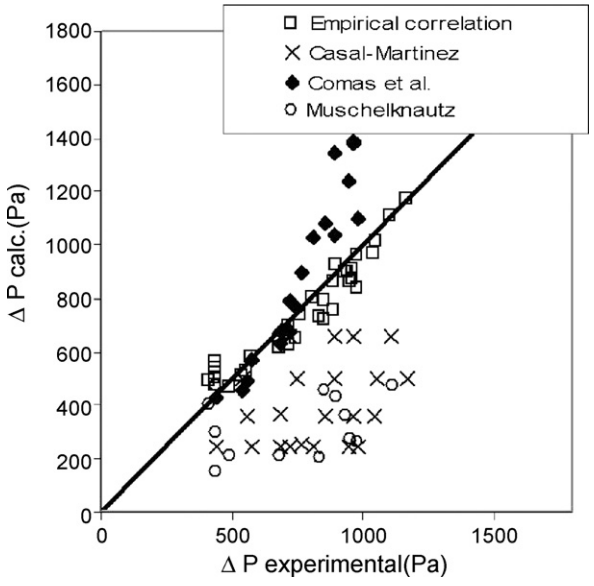

Fig. 2. Cyclone pressure drop calculated by literature models and from the Eq. (6).

where $p_{val,max}$ and p_{cs} are the perimeters of the projection of the openings, on a plane perpendicular to the tube axys, when the valve is completely open, and in the case of partial opening of the butterfly, respectively. In this second case, the cross-section available for the flow is A_{cs}, A_{RD} corresponds to the area of the solid return duct.

When the valve is completely open, $p_{val,max}$ can be calculated as follows:

$$p_{val,max} = D_b \cdot (\pi + 2) \tag{8}$$

where D_b is the butterfly diameter. At an intermediate degree of opening, p_{cs} can be calculated as follows:

$$p_{cs} = D_b \cdot \pi + 2 \cdot \pi \cdot \left\{ 0.5 \cdot \left[\left(\frac{D_b}{2} \right)^2 + \left(\frac{D_b}{2} \cdot \cos\beta \right)^2 \right] \right\}^{0.5} \tag{9}$$

where β is the angle of opening of the butterfly valve; it should be noted that $\beta = 0$ indicates that the valve is completely closed. Using the dimensionless parameter γ, according to Grieco and Marmo [11], the pressure drop in the butterfly valve can be obtained from:

$$\Delta P_{val} = 0.66 \cdot \gamma^{-0.48} \cdot \left(\frac{A_{RD}}{A_{cs}} \right)^{1.2} \cdot \frac{\dot{m}_s}{A_{RD}} \tag{10}$$

3.4. Pressure drop in the return duct

Pressure losses in the solid return duct and in the valve are due to the flowing of gas through the particles. If the voidage, as well as the solid and gas velocities, are known, pressure losses can be calculated by means of the Ergun [27] equation. The solid and gas velocities near the valve vary due to the different cross-sections of the duct and the valve orifices, therefore Leung and Jones [9] found an empirical correlation (Eq. (11)) for pressure drops upstream of the valve (according to the solid motion), introducing an equivalent length into the Ergun equation. By means of Eq. (11) and by imposing ΔP_{val}, it is possible to calculate the gas–solid slip velocity, which is required to calculate the pressure drop in the duct upstream of the valve [1,3,9].

$$\Delta P_{val} = -\left[\frac{150 \cdot \mu \cdot (1-\varepsilon_{mf})^2}{(d_p \cdot \varepsilon_{mf})^2} \cdot \frac{D_{val}}{4} + \frac{1.75 \rho_g \cdot (1-\varepsilon_{mf})}{d_p \cdot \varepsilon_{mf}} \cdot \frac{D_{val}}{24} \cdot |U_{sl,val}| \right] \cdot U_{sl,val} \tag{11}$$

$$\Delta P_{RD} = -\left[\frac{150 \cdot \mu \cdot (1-\varepsilon_{mf})^2}{(d_p \cdot \varepsilon_{mf})^2} + \frac{1.75 \cdot \rho_g \cdot (1-\varepsilon_{mf})}{d_p \cdot \varepsilon_{mf}} \cdot |U_{sl,RD}| \right] \cdot U_{sl,RD} \cdot L_{RD} \tag{12}$$

where $U_{sl,val}$ and $U_{sl,RD}$ are the slip velocities (corresponding to the difference between the gas and solid velocities) in the valve orifices and in the return duct respectively, and D_{val} is the diameter of the valve orifices.

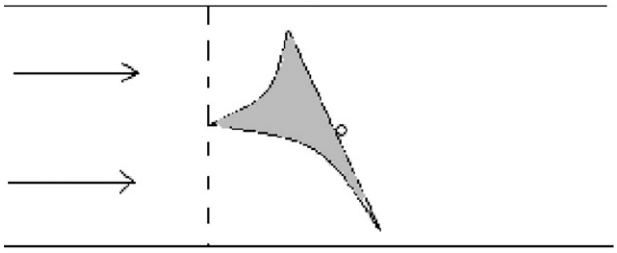

Fig. 3. Cross-section area available for solid flux in front of the butterfly.

A very poor agreement was found when this approach was applied to the experimental apparatus probably due to the very different geometry of the butterfly valve openings compared to a circular orifice.

The model was modified according to the hypothesis that there is a zone in front of the butterfly valve, where the solid is motionless, therefore the cross-section for the passage of the solid tends to reduce gradually from the return duct to the valve openings (Fig. 3).

The space in front of the butterfly valve was divided into a huge number (n) of thin control volumes, characterized by different cross-section.

It was considered that the section available for the solid flow reduces to the same extent along the duct axis, according to a parabolic law as the control volume is close to the valve; the reduction begins at a distance from the butterfly centre equal to the half of the solid duct diameter ($0.5 \times D_{RD}$).

Some preliminary analyses showed that the slip velocities required to find an experimental ΔP_{RD}, by means of Eq. (12), are always much more than the real minimum fluidization velocity, which means the particles are obstructed by their reciprocal interaction, and are in a more similar condition to the packed bed than to the minimum fluidization. According to this consideration, the existence of the region upstream of the valve was postulated where the solid holdup is similar to a packed bed (ε_{pb}).

An initial approximation of the gas flow through the valve ($\dot{V}_g$) is needed to solve the model. The pressure drop in the valve was calculated by means of a step-by-step procedure, which resolves each control volume according to the solid motion, starting from a distance upstream of the butterfly equal to $0.5\,D_{RD}$.

The initial conditions were:

$$v_{g,1} = \frac{\dot{V}_g}{\varepsilon_{pb} \cdot A_{RD}} \qquad v_{s,1} = \frac{\dot{m}_s}{\rho_p \cdot (1-\varepsilon_{pb}) \cdot A_{RD}} \tag{13}$$

where $v_{g,1}$ and $v_{s,1}$ are the gas and solid velocities in the first calculus volume, and A_{RD} is the area of the duct before the valve.

The calculus continues imposing the cross-section available for solid and gas flows for the ith control volume. The cross-section as a parabolic function of the distance from the butterfly

can be calculated from Eq. (14):

$$A_i = \left[\frac{A_{cs} - A_{RD}}{(D_{RD}/2)^2}\right] \cdot \left(\frac{D_{RD}}{2 - x_i}\right)^2 + A_{RD} \quad (14)$$

where x_i is the distance from the butterfly centre.

The gas and solid velocities in the ith control volume can be calculated according to the continuity equation by means of Eqs. (15) and (16).

$$v_{g,i} = \frac{\dot{V}_g}{\varepsilon_{pb} \cdot A_i} \quad (15)$$

$$v_{s,i} = \frac{\dot{m}_s}{\rho_p \cdot (1 - \varepsilon_{pb}) \cdot A_i} \quad (16)$$

The gas–solid slip velocity correspond to:

$$U_{sl,i} = v_{g,i} - v_{s,i} \quad (17)$$

The pressure drop in the ith control volume is:

$$\Delta P_i = \left[\frac{150 \cdot \mu \cdot (1 - \varepsilon_{pb})^2}{(d_p \cdot \varepsilon_{pb})^2} + \frac{1.75 \cdot \rho_g \cdot (1 - \varepsilon_{pb})}{d_p \cdot \varepsilon_{pb}} \cdot |U_{sl,i}|\right] \cdot U_{sl,i} \cdot vt \quad (18)$$

The solution is calculated for the n control volumes, and the total pressure drop (ΔP_{cal}) is obtained as $\sum_1^n \Delta P_i$. The procedure is then repeated varying $\dot{V}_g$ until

$$\Delta P_{cal} = \Delta P_{val} \quad (19)$$

The value of ΔP_{val} to be introduced in Eq. (19) is calculated directly as a function of the solid circulation rate by mean of Eq. (10).

Since the voidage upstream of the valve is different from the one in the standpipe, a change in ε occurs along the duct that connects the standpipe to the butterfly valve. According to the Ergun [27] equation, it is possible to calculate the pressure drop in the duct by numerical solution of Eq. (20).

$$\Delta P_{RD} = \int_0^{L_{RD}} \left[\frac{150 \cdot \mu \cdot (1 - \varepsilon)^2}{(d_p \cdot \varepsilon)^2} + \frac{1.75 \cdot \rho_g \cdot (1 - \varepsilon)}{d_p \cdot \varepsilon} \cdot |v_g - v_s|\right] \cdot (v_g - v_s) dx \quad (20)$$

Eq. (20) requires the knowledge of the profile of ε along the duct, but, according to the model, only the voidage in the standpipe and immediately upstream of the valve are known, therefore a linear reduction in the voidage from ε_{mf} to ε_{pb} was imposed. As this assumption has no justification, a parabolic profile was also tested and as linear and parabolic profiles lead to similar values of ΔP_{RD}, the linear one was chosen.

In Figs. 4 and 5, corresponding respectively to inventory of 20.1 and 36.3 kg, the values of ΔP_{RD} calculated by mean of Eqs. (11) and (12), and by mean of the new model are compared. In the latter case, the agreement with the experimental data is very good. With higher inventories (Fig. 5) the pressure drop in the valve and in the solid duct are much higher, and the model brings to good results in both cases.

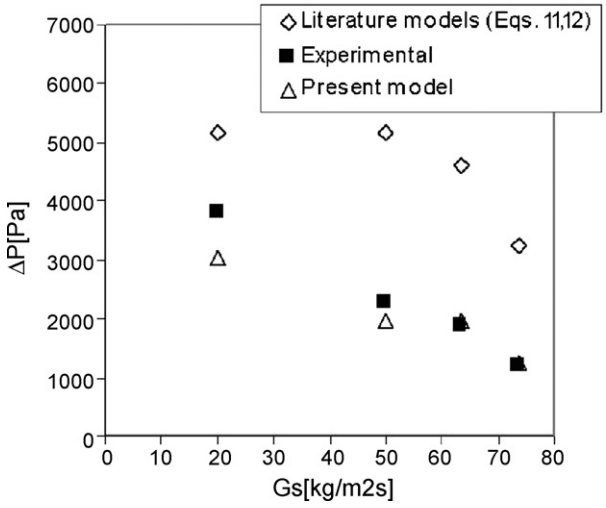

Fig. 4. Comparison of the return leg pressure drop calculated with the present model and by literature models (Eqs. (11) and (12)), inventory 20.1 kg.

3.5. Pressure drop in the duct connecting riser top to the cyclone

Most of the literature models that perform a pressure balance in the solid circulation loop [1–3] neglect the pressure drop in the duct between the riser exit top and the cyclone. This approximation is valid when the plant works in fast fluidization conditions because the pressure drop in this duct is much smaller than ΔP_R. Under lean conditions, in pneumatic transport, the pressure drop in the bend at the top of the riser can be an important fraction of the riser one (Table 2).

Experimental results have shown that the pressure drop is mainly due to the curve at the top of the riser, and the contri-

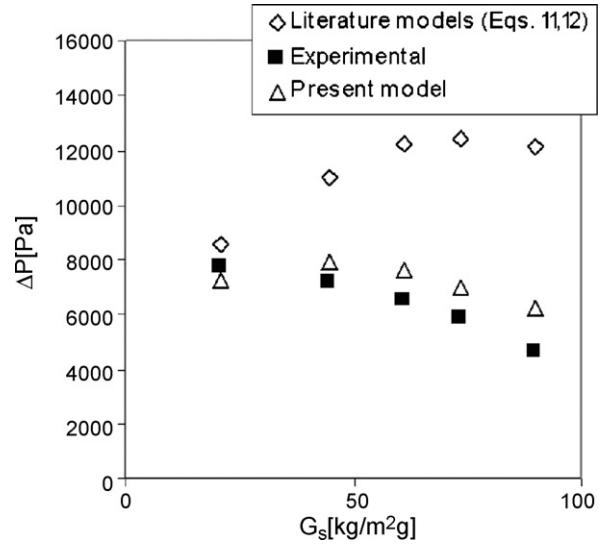

Fig. 5. Comparison of the return leg pressure drop calculated with the present model and by literature models (Eqs. (11) and (12)), inventory 36.3 kg.

Table 2
Working conditions and results of the pressure balance for the whole solid circulation loop

Working conditions	Case 1		Case 2		Case 3		Case 4		Case 5	
A_{val} (m^2)	0.000395		0.00117		0.00121		0.00231		0.00211	
U_0 (m/s)	2.1		2.06		2.1		2.6		3.1	
G_s (kg/m^{2}s)	34.31		56.199		35.8		56.7		73.7	
Inventory (kg)	36.3		36.3		20.09		20.09		20.09	
Results	Calc.	Exper.	Calc.	Exper.	Calc.	Exper.	Calc.	Exper.	Calc.	Exper.
U_R (m/s)	2.3	/	2.16	/	2.18	/	2.69	/	3.19	/
F_{RD} (m^3/h)	5.36	/	2.98	/	1.84	/	2.21	/	2.53	/
ΔP_R (Pa)	2,491	2,943	6,775	6,523	2,549	2,285	2,490	2,658	2,450	2,678
ΔP_{RD} (Pa)	6,351	5,984	2,389	2,746	1,422	1,883	1,335	1,393	1,244	1,177
ΔP_{val} (Pa)	3,449	3,335	983	931	594	588	524	313	501	470
ΔP_{UD} (Pa)	919	902	1,178	922	962	980	1,031	961	988	863
ΔP_{cy} (Pa)	561	441	5,719	618	558	441	749	794	928	931
ΔP_{SP} (Pa)	13,772	13,998	12,047	12,265	6,106	6,265	6,130	6,268	6,146	6,265

bution of the horizontal duct to the ΔP_{UD} is always negligible, although some researchers consider this term in the pressure balance [7].

The curve pressure drop can be calculated with the model found in [28], but this approach showed very poor results in the present case, and as a consequence, an empirical correlation was developed to calculate ΔP_{UD} as a function of the gas and solid flow rate.

$$\Delta P_{UD} = (202.5 \cdot U_g + 1288.5) \cdot \times[1 - \exp(-0.0307 \cdot U_g^{0.732} \cdot G_s)] \quad (21)$$

3.6. Calculation of the riser holdup profile

According to Eq. (22):

$$\Delta P_R = \Delta P_{SP} - \Delta P_{cy} - \Delta P_{RD} - \Delta P_{val} - \Delta P_{UD} \quad (22)$$

ΔP_R is calculated imposing the closure of the pressure balance. Since ΔP_R is mainly due to the solid holdup and wall friction, we obtain:

$$\int_0^{z_R} [g \cdot \rho_p(1-\varepsilon) + f]dz = \Delta P_R \quad (23)$$

In most cases, the importance of the wall friction term is quite limited, therefore, due to the uncertainty found when applying literature correlations for wall friction, we decided to neglect f.

Solid holdup profiles have different shapes that depend on the fluid-dynamics regime. The Bai–Kato [12] correlation (Eq. (24)) was used, since it can predict the value of G_S at which a dense zone begins to form at the bottom of the column.

$$G_s^* = 0.125 \cdot \frac{\mu}{d_p} \cdot Fr^{1.85} \cdot Ar^{0.63} \cdot \left(\frac{\rho_p - \rho_g}{\rho_g}\right)^{-0.44} \quad (24)$$

where Fr and Ar are the Froude and the Archimede numbers, which are calculated as:

$$Fr = \frac{U_R}{(g \cdot d_p)^{0.5}} \quad Ar = \frac{d_p^3 \cdot \rho_g \cdot (\rho_s - \rho_g) \cdot g}{\mu^2}$$

In the transport regime, the solid holdup is postulated to decay from the bottom to the top of the riser following an exponential law, therefore we obtain:

$$\varepsilon_p = \exp(-a \cdot z) \cdot (\varepsilon_{p,z=o} - \varepsilon_{p,\infty}) + \varepsilon_{p,\infty} \quad (25)$$

Only two ($\varepsilon_{p,\infty}$, the asymptotic value of the voidage ta infinite height, and a, the exponential decay coefficient) of the three parameters in Eq. (25) could be calculated according to literature correlations, the third ($\varepsilon_{p,z=0}$, the voidage at the riser bottom) was determined imposing the closure of the pressure balance (23).

In order to calculate $\varepsilon_{p,\infty}$, Wong et al. [13] and Bai and Kato [14] models were tested: the first seemed to match the experimental results more closely, therefore, according to Wong et al. [13], we posed:

$$\varepsilon_{p,\infty} = 1 - \frac{U_R \cdot \rho_p}{2 \cdot G_s + U_R \cdot \rho_p} \quad (26)$$

In order to calculate the decay coefficient (a) the Lei–Horio [1] correlation was used:

$$a = 0.019 \cdot \left(\frac{G_s}{U_R \cdot \rho_g}\right)^{-0.22} \cdot \left(\frac{U_R}{\sqrt{g \cdot D_R}}\right)^{-0.32} \cdot \times \left(\frac{\rho_p - \rho_g}{\rho_g}\right)^{0.41} \cdot \frac{1}{D_R} \quad (27)$$

The existence of a dense zone at the bottom was assumed when the riser was in the fast fluidization regime. The voidage in the dense zone was assumed to be constant with the height, and an exponential solid concentration decay was assumed downstream of the dense zone.

The most critical aspect when predicting the riser behaviour in this regime is the calculus of the height of the dense zone,

which is again done by imposing Eq. (23). The void fraction in the dense zone can be calculated by means of the Bai–Kato [14] correlation (Eq. (28)):

$$\varepsilon_{p,z=0} = \left[1 + 0.103 \cdot \left(\frac{U_R}{(G_s/\rho_p)}\right)^{1.13} \cdot \left(\frac{\rho_p - \rho_g}{\rho_g}\right)^{-0.013}\right] \cdot \times \left(\frac{G_s}{[\rho_p \cdot (U_R - U_t]}\right) \quad (28)$$

The solid holdup profile in the upper zone is calculated using Eq. (29), which is an adjustment of Eq. (25)

$$\varepsilon_p = \exp(-a \cdot z + a \cdot z_d) \cdot (\varepsilon_{p,z=0} - \varepsilon_{p,\infty}) + \varepsilon_{p,\infty} \quad (29)$$

where a, $\varepsilon_{p,\infty}$ and $\varepsilon_{p,z=0}$ are calculated according to Eqs. (26)–(28), respectively. The height of the dense zone is varied in order to verify Eq. (23).

3.7. Numerical solution and coupling between mass and pressure balance

Combining Eqs. (22) and (23), neglecting the friction, one obtains:

$$W_R = \frac{(\Delta P_{SP} - \Delta P_{cy} - \Delta P_{RD} - \Delta P_{val} - \Delta P_{UD}) \cdot A_R}{g} \quad (30)$$

Eq. (30) has to be satisfied together with Eq. (5). This can be achieved by means of a simple iterative process starting from an estimate of ΔP_R (initial value can be even 0) and applying Eq. (5) first, and then Eq. (30), until the model converges to a solution of W_R (or ΔP_R) able to satisfy both the conditions. This process warrants that both mass and pressure balances are respected.

Each iteration requires the calculation of most of the terms corresponding to the pressure losses along the loop.

The amount of solid present in the cyclone and in the upper duct are neglected, W_{RD}, the mass of solid present in the return leg, is directly calculated being known the geometry and the void fraction distribution.

4. Results and discussion

The results of the balance are shown in Figs. 6–10. The model has proved to be able to predict the holdup profile even in the case of a very low solid flux. Since the ΔP_R under lean conditions is small, a small absolute error in the calculation of the pressure drops of the other sections of the plant can result in a great relative error on ΔP_R, and this can lead to important over or under prediction of ΔP_R and hence of the holdup profile.

As demonstrated by Figs. 6–10, the model predicts the holdup profile at as low G_S as 35 kg/m^{2}s. Table 2 contains the model results for the whole loop.

As a general consideration, from the Table 2 it is clear that the model can predict with high accuracy the pressure drop of each component of the loop under a wide range of experimental conditions. Even under very lean operative conditions each of the pressure drop caused by the loop components (valve, bend, return duct, etc.) is accurately predicted. In particular, the valve pressure drop is very accurate under each condition. The standpipe pressure drop is easily predictable, being due to a certain amount of solid at minimum fluidization condition. However, since ΔP_{SP} is the maximum value that appears in Eq. (22), the maximum precision is needed to avoid affecting the calculation of ΔP_R. This result is achieved in this work because of the high precision in the closure of the coupled mass and pressure balance.

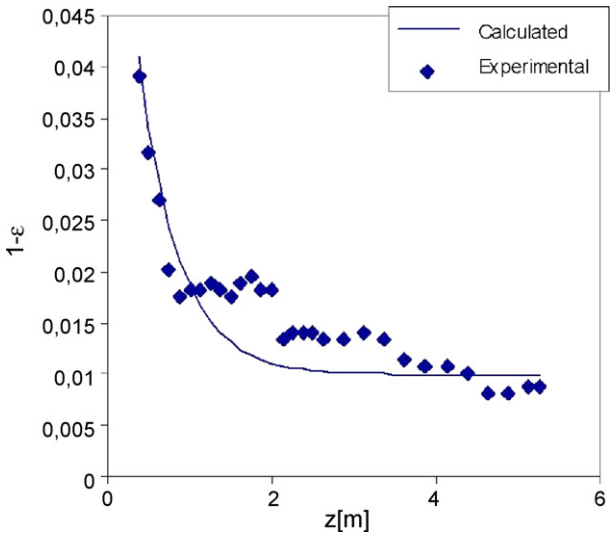

Fig. 6. The results of the model: solid circulation loop pressure losses and riser holdup axial profile, case 1.

As a consequence, very good predictions of the riser pressure drop, and hence of the axial holdup profiles are obtained. Basically the ΔP_R is predicted within 10% of the real value, except for case 1. For each case the main errors in the pressure

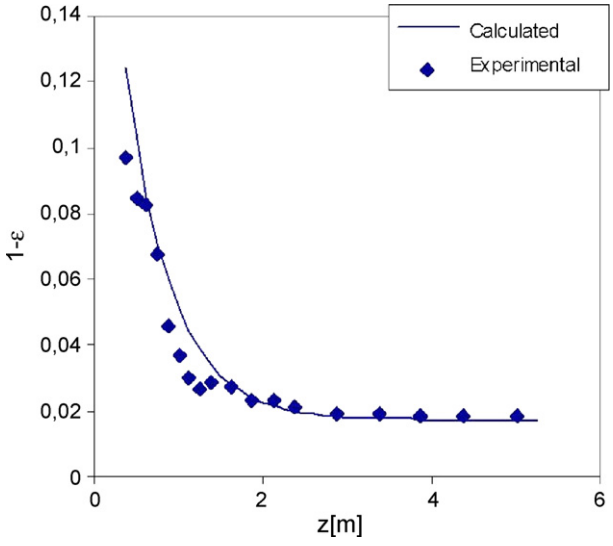

Fig. 7. The results of the model: solid circulation loop pressure losses and riser holdup axial profile, case 2.

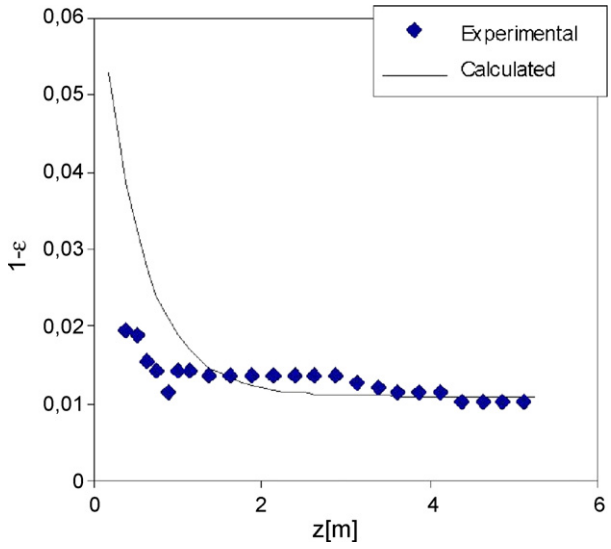

Fig. 8. The results of the model: solid circulation loop pressure losses and riser holdup axial profile, case 3.

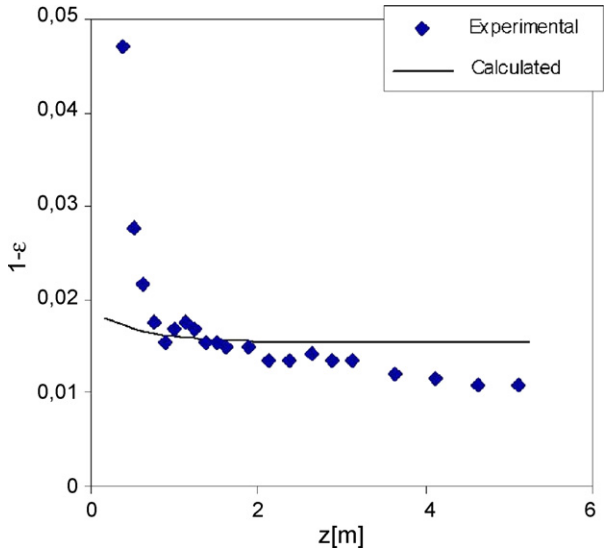

Fig. 10. The results of the model: solid circulation loop pressure losses and riser holdup axial profile, case 5.

balance arises from the prediction of ΔP_{RD} that represent one of the higher values of the ΔP appearing in the pressure balance. It is the opinion of the authors that further work should be done to improve the axial voidage profile in the valve and in the solid return duct (RD), to improve the modelling of this section.

In Fig. 8, the difference between calculus and experimental results is due in particular to the fact that the total riser pressure drop estimated from the pressure balance is about 10% higher and the holdup calculated in the final part of the riser is right, as a consequence the errors are concentrated on the first part of the riser and the decay factor was underestimated.

Cases 4 and 5 (Figs. 9 and 10) are affected in particular by an overestimate of $\varepsilon_{p,\infty}$ that in case 5 can reach even 35%. In this case, the model, in order to obtain from the holdup profile the same pressure drop given by the pressure balance, had to reduce strongly the decay factor bringing to a flat holdup profile.

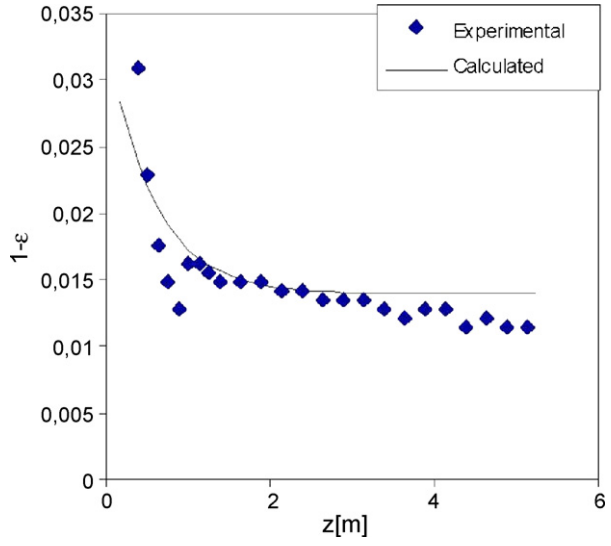

Fig. 9. The results of the model: solid circulation loop pressure losses and riser holdup axial profile, case 4.

5. Conclusions

A model has been developed to calculate the pressure balance in the loop of a circulating fluidized bed equipped with a butterfly valve as a solid flux controlling device. The input variables of the models are the geometrical features of the riser, the solid flux and the gas superficial velocity.

The model can predict with high accuracy the pressure drop across each component of the loop. This result was obtained since ad hoc models have been developed for the prediction of the ΔP in the butterfly valve, in the duct connecting standpipe and valve, in the bend after the riser and in the cyclone.

The model allows the riser pressure drop to be predicted via the closure of the pressure balance. Since the ΔP_R is predicted with high accuracy, it can be used to predict the axial holdup profile of the riser. A good agreement with the experimental results was obtained even for very low G_S.

The application of this model to generalized geometries requires the validation of the correlations used for cyclone and bend pressure drops. Definitely the prediction of the behaviour of CFB by pressure balance still requires the development of specific sub-models for cyclones and return lines, as the working conditions in these parts are often too different from the one used to develop general purpose models or correlations presented in literature. On the other hand, the models presented in this paper for valve and connecting duct pressure drop prediction have a higher generality, being less empirical and represent a step toward the construction of a generalized model for the pressure balance of a CFB.

References

[1] H. Lei, M. Horio, A comprehensive pressure balance model of circulating fluidized beds, Journal of Chemical Engineering of Japan 31 (1998) 83–94.

[2] L. Cheng, P. Basu, Effect of pressure on loop seal operation for a pressurized circulating fluidized bed, Powder Technology 103 (1999) 203–211.

[3] L. Cheng, P. Basu, K. Cen, Solids circulation rate prediction in a pressurized loop seal, Chemical Engineering Research & Design 76 (1998) 761.

[4] D. Bai, J. Issangya, J.R. Grace, Analysis of the overall pressure balance around a high-density circulating fluidized bed, Industrial Engineering Chemistry Research 36 (1997) 3898–3903.

[5] K.S. Lim, P. Peeler, R. Close, T. Joyce, Estimation of solids circulation rate in CFB from pressure loop profiles, in: J. Werther (Ed.), Circulating fluidized bed Technology VI, DECHEMA, Frankfurt, Germany, 1999, p. 455.

[6] M.J. Rhodes, D. Geldart, A model for circulating fluidized bed, Powder Technology 53 (1987) 155.

[7] S.W. Kim, S.D. Kim, D.H. Lee, Pressure balance for circulating fluidized beds with a loop seal, Industrial Engineering Chemistry Research 41 (2002) 4949–4956.

[8] W.C. Yang, A model for the dynamics of a circulating fluidized bed loop, in: P. Basu, J.F. Large (Eds.), Circulating Fluidized Bed Technology II, Pergamon Press, Oxford England, 1988, p. 181.

[9] L.S. Leung, P.J. Jones, in: J.F. Davidson (Ed.), Coexistence of Fluidized Solids Flow and Packed Bed Flow in Stand-Pipes, Fluidization, Academic Press, 1985, p. 297.

[10] J.A.H. De Jong, Q.E.J.J.M. Hoelen, Concurrent gas and particle flow during pneumatic discharge from a bunker through an orifice, Powder Technology 12 (1975) 201–208.

[11] E. Grieco, L. Marmo, A correlation for pressure drop versus mass flow in a butterfly control valve of a circulating fluidized bed, Powder Technology 161 (2) (2006) 89–97.

[12] D. Bai, K. Kato, On saturation carrying capacity of gas, Journal of Chemical Engineering of Japan 28 (2) (1995) 179.

[13] R. Wong, T. Pugsley, F. Berruti, Modelling the axial voidage profile and flow structure in risers of circulating fluidized beds, Chemical Engineering Science 47 (1992) 2301–2306.

[14] D. Bai, K. Kato, Quantitative estimation of solids holdups at dense and dilute regions of circulating fluidized beds, Powder Technology 101 (1999) 183–190.

[15] D. Geldart, Types of gas fluidization, Powder Technology 7 (1973) 185–195.

[16] W.C. Yang, A model for dynamics of circulating fluidized bed loop, in: P. Basu, J.F. Large (Eds.), Circulating Fluidized Bed Technology II, Pergamon Press, Oxford, 1988.

[17] J.M. Martinez, J. Casal, Optimization of parallel cyclones, Powder Technology 38 (1984) 217–221.

[18] E. Muschelknautz, K. Brunner, Untersuchungen an Zyklonen, Chemie-Ing.-techn. 39 (1967) 531–538.

[19] M. Comas, J. Comas, C. Chetrit, J. Casal, Cyclone pressure drop and efficiency with and without inlet vane, Powder Technology 66 (1991) 143–148.

[20] J. Chen, M. Shi, A universal model to calculate cyclone pressure drop, Powder Technology 171 (2007) 184–191.

[21] B. Zhao, A theoretical approach to pressure drop across cyclone separators, Chemical Engineering Technology 27 (2004) 1105–1108.

[22] J.A.H. De Jong, Vertical air-controlled particle flow from a bunker trough circular orifices, Powder Technology 3 (1969) 279–286.

[23] D.R.M. Jones, J.F. Davidson, The flow of particles from a fluidised bed through orifices, Rheologica Acta 4 (1965) 180.

[24] M.R. Judd, P.D. Dixon, The flow of dense solid down a vertical stand-pipe, in: AIChE Annual Conference, Chicago, December, 1976.

[25] Y. Jin, Z.W. Wang, J.X. Zhu, Z.Q. Yu, A study of particle flow between fluidized beds, in: M. Kwauk, D. Kunii (Eds.), Fluidization '85—Science and Technology, Science Press, Beijing, 1985, pp. 172–183.

[26] M. Kuramoto, D. Kunii, T. Furusawa, Flow of dense fluidized particles through an opening in a circulation system, Powder Technology 47 (2) (1986) 141.

[27] S. Ergun, Fluid flow trough packed columns, Chemical Engineering Process 48 (1952) 89.

[28] D. Kunii, O. Levenspiel, Fluidization Engineering, Kieger Publishing Co., Huntington, NY, 1977.